

Chapter 3

Fabrication and Characterization of *n*-Si(111) Based Metal-Insulator-Semiconductor Diodes

1. Introduction

Our knowledge of metal-semiconductor diodes goes back more than a century ago when Braun,¹ in 1874, discovered the rectifying nature of metallic contacts on semiconductors such as copper, iron, and lead sulfide crystals.² It was not until 1931, when Schottky³ proposed the existence of some sort of potential barrier at the metal-semiconductor contact, that the scientists began to understand the rectifying nature of this junction. In 1938, Schottky⁴ and Mott⁵ pointed out, independently, that the potential barrier formation was the result of a difference between the work functions of the metal and semiconductor, and the metal-semiconductor barrier height (ϕ_b) could be calculated according to this equation:

$$\phi_b = (\varphi_m - \chi_s) / q \quad (3.1)$$

where φ_m is the metal work function and χ_s is the electron affinity of the semiconductor. This behavior has come to be known as the “Schottky limit.”

Practical metal-semiconductor contacts do not always appear to obey the Schottky limit. Linear dependence of the barrier height on metal work function is predominantly observed in ionic semiconductors only. In the case of covalent semiconductors, some have barrier heights that are only weakly dependent on φ_m , and some exhibit almost no relationship between ϕ_b and φ_m .⁶ Bardeen⁷ was the first to point out the importance of localized surface states, which exist in many covalent semiconductors, in determining the barrier height. These surface states arise from the dangling bonds at the semiconductor surface where no neighboring atoms are available for making covalent bond on the vacuum side, and their energies are usually continuously distributed across the bandgap. When brought into contact with a metal, equilibration between Fermi levels of these two phases occurs first by exchanging charges between the metal and the surface states,

which then reduces or eliminates the effect on the semiconductor depletion region.² As a result the barrier height is primarily determined by the surface states and is largely independent of the metal in contact. A system that obeys this “Bardeen limit” is described as “Fermi-level pinned.”

Heine⁸ argued that when a metal is deposited on a semiconductor surface, it is possible for the wave function of electrons in the metal with energies corresponding to the forbidden gap in the semiconductor to extend into the semiconductor and thereby induce states within the bandgap. These metal induced gap states (MIGS) replace the intrinsic electron states that may be present on the semiconductor surface, and can affect the true barrier height measurements.

In some cases, when a metal is deposited on a semiconductor surface, an interfacial reaction between the metal and the semiconductor occurs to form deleterious silicide. This interfacial reaction causes the interface to move into the semiconductor bulk, and as a result the barrier height is independent of the surface properties and the metal work function.^{9-11,12,13} It was found that the barrier heights of this type of MS contacts are linearly dependent on the heat of formation of the silicide.¹⁴ In these cases the properties of the silicides controls barrier formation, which prevents the true barrier height of the MS contacts to be determined.

A thin-film insulator, namely thermally grown oxide, has been used to make metal-insulator-semiconductor (MIS) contacts since the mid-60’s. A native thin oxide layer on the semiconductor surface is thin enough that a significant number of electrons can tunnel through it, and it also satisfies the dangling bonds and thus reduces the intrinsic surface state density. However, thermally grown oxides on silicon typically contain fixed positive charges, which increase the barrier height of *p*-type Si junctions, but have an opposite effect on *n*-type Si junctions.¹⁵ Some metals can also penetrate through a thin layer of oxide, and react with the semiconductor to form silicide. Although it’s now possible to control oxide layer thicknesses on the order of angstroms,

oxide layers tend to grow thicker over time and consequently lower the current that was allowed to tunnel through.

An alkyl monolayer can serve as a useful alternative to the oxide layer in MIS devices, because its thickness is easily controlled down to an atomic level. Since such layers can be covalently attached to the Si surface, they also satisfy the dangling bonds and reduce the density of surface states. Since the interactions between the independent alkyl chains and the Si atoms are covalent, they can align themselves in registry with the Si atoms better than the lattice-constrained oxygen atoms in SiO₂. Many alkyl groups have been covalently attached to Si(111) surfaces via a two-step chlorination/alkylation procedure.¹⁶⁻¹⁸ This modification technique could be utilized to develop a MIS system enabling barrier height measurements of intimate metal-semiconductor contacts not currently possible. For an improved MIS system with an alkyl insulating layer, the observed ϕ_b value should be closer to the Schottky limit. Another advantage of using an alkyl insulator is that the thickness is easily controlled by using different chain lengths, and thus reproducible thicknesses can be achieved for systematic investigation of its effects on the junction electrical properties. Barrier height measurements and $J-E$ characterization of the MIS with different insulator thickness could identify an optimal alkyl chain that can effectively inhibit silicide formation while introducing the minimal series resistance.

Introduction of a thin insulating layer between a metal and a semiconductor could affect the $J-E$ characteristics of an MS contact in many ways. An insulating layer could reduce the number of majority carriers crossing the interface from the semiconductor into the metal, decrease the reverse saturation current density (J_0), and therefore increase the open-circuit voltage (V_{oc}). It could also act as a chemical barrier and prevent unfavorable interfacial reactions between the metal and the semiconductor. As depicted in Figure 3.1, voltage drop typically occurs at a MIS interface due to the resistance of the insulator. However, when the insulating layer is very thin (i.e., $< 20 \text{ \AA}$), the potential drop across it

should be negligibly small compared to that in the semiconductor depletion region,² and electrons should be able to tunnel through this layer relatively easily. Straight alkyl chains tend to line up on a surface and form an organized overlayer, which will also encourage electron tunneling. In this case, the barrier height and the contact potential difference should be unaffected by the presence of the thin interfacial layer, and the true MS barrier height can be extracted for silicide-forming metal/Si interfaces.

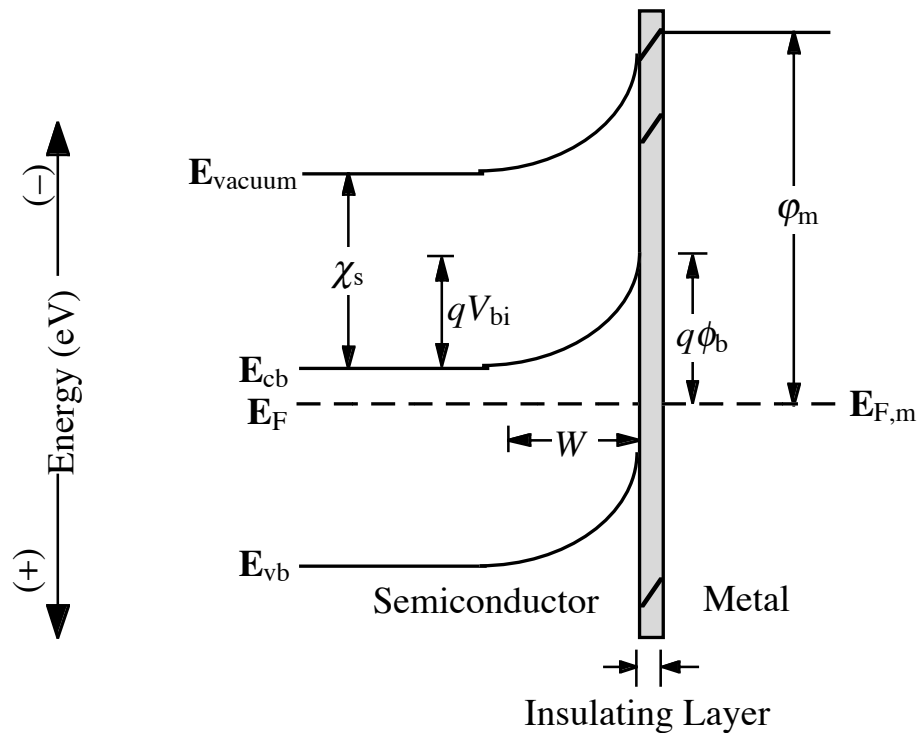


Figure 3.1

A band bending diagram of a metal-insulator-semiconductor (MIS) junction. The barrier height (ϕ_b) of this junction is less than the difference between the metal work function (ϕ_m) and the electron affinity of the semiconductor (χ_s), and it is caused by a voltage drop across the insulating layer. If the insulating layer is thin enough, the voltage drop can become negligible, and can mimic the electrical properties of the equivalent metal/semiconductor junction.

2. Experimental

2.1. Solvents and Reagents

All solvents used for surface modification, including anhydrous methanol, anhydrous chlorobenzene, anhydrous acetonitrile, and anhydrous tetrahydrofuran (THF) were obtained from Aldrich and were used as received. These solvents were packaged under $N_2(g)$ in Sure/Seal bottles and were stored over activated 3 Å molecular sieves (EM Science) in a $N_2(g)$ -purged glove box. Solvents used for wafer degreasing, acetone, dichloromethane, methanol, and 1,1,1-trichloroethane, were either reagent grade (GR) or Omnisolve grade obtained from EM Science and used as received. The 30% H_2O_2 was purchased from EM Science, and the $H_2SO_4(aq)$ was obtained from J. T. Baker. Hydrofluoric acid buffered with ammonium fluoride (NH_4F/HF , buffered HF) and 40% ammonium fluoride (NH_4F) solutions were purchased from Transene Co. The 18 $M\Omega\cdot cm$ resistivity H_2O was collected from a Barnstead E-pure filtration system. The following chemicals used for surface modification were purchased from Aldrich and were used without further purification: Phosphorus pentachloride (PCl_5), benzoyl peroxide, methylmagnesium bromide (CH_3MgBr , 3.0 M in diethyl ether), methylmagnesium chloride (CH_3MgCl , 3.0 M in THF), ethylmagnesium bromide (C_2H_5MgBr , 3.0 M in diethyl ether), propylmagnesium chloride (C_3H_7MgCl , 2.0 M in diethyl ether), butylmagnesium chloride (C_4H_9MgCl , 2.0 M in THF), hexylmagnesium bromide ($C_6H_{13}MgBr$, 2.0 M in diethyl ether), octylmagnesium chloride ($C_8H_{17}MgCl$, 2.0 M in THF), and decylmagnesium bromide ($C_{10}H_{21}MgBr$, 1.0 M in diethyl ether).

2.2. Semiconductor Material and Etching

Single-crystal, (111)-oriented *n*-type silicon wafers with a polished front side were obtained from Crysteco. The wafers were phosphorous-doped with a resistivity of 2–8.5 Ω ·cm and a thickness of 475–550 μ m as specified by the manufacturer. The silicon wafers were first oxidized in a “Pirhana” solution which consisted of 3:1 (v/v) concentrated $\text{H}_2\text{SO}_4(\text{aq})$: H_2O_2 (30%) heated to approximately 100 °C for one hour.¹⁸

Caution: *The acidic “Pirhana” solution is extremely dangerous, particularly in contact with organic materials and should be handled carefully.* The wafers were then rinsed with copious amount of 18.0 M Ω ·cm resistivity water (obtained from a Barnstead Inc. Nanopure water purification system), dried under pressurized $\text{N}_2(\text{g})$, and stored for future use. Ohmic contact was made by rubbing an Ga-wetted In ball on the non-polished side of both derivatized and H-terminated samples. This was done by first rubbing an In (99.999%, Alfa Aesar) ball into a small amount of melted Ga (99.99+%, Aldrich) to create a eutectic mixture. An In ball, held by a tweezer, was then dipped into and wetted by the eutectic mixture, and was used to rub on the back side of the Si samples.

Before surface modifications, the wafer was cut into smaller size samples. Each piece was briefly sonicated in 18.0 M Ω ·cm resistivity water, degreased by rinsing sequentially with methanol, acetone, 1,1,1-trichloroethane, dichloromethane, 1,1,1-trichloroethane, acetone, and methanol, and followed by another brief sonication in water. After blow drying with $\text{N}_2(\text{g})$, the samples were etched in $\text{NH}_4\text{F}/\text{HF}$ (buffered HF) for 30–45 seconds, and then without rinsing immersed in 40% NH_4F for 10–15 min.¹⁹ Tiny bubbles were observe to appear on the (111) surface of the samples when immersed in 40% NH_4F . Following the etching process, the samples were rinsed with 18.0 M Ω ·cm resistivity water (obtained from Barnstead E-pure filtration system), and dried under a stream of $\text{N}_2(\text{g})$. The samples were quickly mounted onto the XPS stubs and introduced

into ultrahigh vacuum (UHV) system that houses the x-ray photoelectron spectroscopy (XPS) via an atmospheric load lock for immediate surface characterization.

2.3. Surface Modification

All surface modification procedures were carried out in a $N_2(g)$ -purged glove box which is connected to the UHV system housing the XPS spectrometer via a gate valve. After verifying the surfaces were H-terminated, the samples were transferred into glove box without exposing to the air. The stock chlorinating solution was prepared by dissolving excess PCl_5 in chlorobenzene to form a saturated solution (typically 0.6–0.7 M). The solution was warmed to about 60 °C for at least 1 hour to ensure that enough PCl_5 had dissolved. Immediately before use, a small portion of the stock chlorinating solution was poured into a small beaker, and a few grains of benzoyl peroxide were added (approximately 30–40 mg of benzoyl peroxide in 10 ml of PCl_5 -chlorobenzene solution) as a radical initiator.^{20,21} With the samples completely immersed in this solution and the beaker covered by a watch glass, the reaction was heated to 90–100 °C for 45–50 min. The samples were then taken out of the chlorinating solution, rinsed with anhydrous THF followed by anhydrous methanol, and dried in a stream of $N_2(g)$. The chlorinated samples were mounted on the stub and transferred into UHV for characterization.

Following the XPS characterization, the chlorinated samples were transferred back into the glove box and further derivatized by alkylation. The samples were immersed in alkyl Grignard ($RMgX$: $R = CH_3, C_2H_5, C_3H_7, C_4H_9, C_6H_{13}, C_8H_{17},$ or $C_{10}H_{21}$; $X = Br$ or Cl) solutions and heated to 65–80 °C. The duration of this step was varied with the alkyl chain length, and is summarized in Table 3.1.²² The alkylated samples were rinsed thoroughly with anhydrous THF followed by anhydrous methanol, individually immersed in anhydrous methanol in screw-capped vials, and taken out of the glove box for sonication. The derivatized samples were sonicated in anhydrous methanol

and anhydrous acetonitrile for 5 min each, dried in a stream of $N_2(g)$ before being mounted on the XPS stub, and introduced into UHV through atmospheric load lock for surface characterization.

Table 3.1

A summary of reaction time, overlayer thickness, and air stability of alkyl-terminated Si.

Alkyl Group	Reaction Time (hr)	Observed Ellipsometric Thickness ^a (Å)	Air Stability ^{a,b} (hr)
CH ₃	2.5 – 8	--	--
C ₂ H ₅	2.5 – 10	7 ± 2	20
C ₃ H ₇	10 – 18	--	--
C ₄ H ₉	12 – 24	9 ± 1	> 87
C ₆ H ₁₃	16 – 46	11 ± 1	> 87
C ₈ H ₁₇	20 – 46	--	--
C ₁₀ H ₂₁	20 – 72	12 ± 2	30

^a The data were taken from prior studies performed in our laboratory.

^b The numbers represent the amount of time for alkyl-terminated surfaces to oxidize in air to an extent that a half monolayer of oxide could be detected by the XPS.

2.4. Metal Deposition and Device Fabrications

2.4.1. The First-Generation MIS Device

Electrodes were fabricated by attaching a tinned copper wire (22 AWG, Belden) to the ohmic contact of unmodified Si using electrically conductive silver print (GC Electronics). As illustrated in Figure 3.2, the wire was encased in glass tubing and the backside and edges of the electrode were sealed with insulating white epoxy (Epoxy Patch Kit 1C, Dexter Corp.), leaving only the polished surface of the crystal exposed. Another thin tinned copper wire was wrapped around the epoxy seal in a close proximity to the Si and the outside of the glass tubing before the epoxy was completely hardened. The electrodes were stored in a covered tray for at least 24 hours for the epoxy to cure. A layer of Ni was then deposited on the front side of electrode, covering the Si and the epoxy surrounding it, along with the thin tinned copper wire that was situated near the Si. The front contact was provided by the deposited metal film that electrically connects the Si surface and the tinned copper wire. A small amount of silver print was painted around the wire and epoxy to ensure a good electrical connection. Electrode areas were determined by digitally scanning the electrodes along with a micro ruler, and the exposed electrode areas were traced and measured using the digitizing software ImageSXM. The typical exposed electrode areas were 0.05–0.15 cm².

All electrodes made of modified Si were transferred to a high-vacuum evaporation chamber (Vacuum Coating Unit LCI-14B, Consolidated Vacuum Corp.) and evacuated to a pressure of $\leq 5 \times 10^{-6}$ Torr. The Ni (99.994%, Alfa AESAR) was deposited onto the electrodes at a rate of 2–5 Å/s to a thickness of ~450 Å by filament evaporation. Evaporation rates and film thicknesses were determined by a R. D. Mathis TM-100 thickness monitor.

2.4.2. The Second-generation MIS Device

The Si wafers were cut into 5 mm × 5 mm pieces and were modified and characterized as described. Immediately following the surface derivatization process, the modified samples were introduced into the evaporator for metal deposition. The thickness of the deposited metal film was usually 450 Å. Figure 3.3 depicts the cell assembly of this sandwiched MIS device. Each device could hold two samples at the same time. Two small Cu plates embedded on the bottom portion of the device provided the back contacts. The ohmic contacted backside of a sample was bonded to the Cu plate using silver print. Two thick Cu wires were inserted into the top portion of the device made of delrin at an angle so that the ends appeared on the surface of the underside near the two circular openings. The wire ends were cut and polished to the level of the delrin top plate surface and referred to as Cu dots. When the cell was assembled, the Cu dots should touch the samples and make electrical contacts with the deposited metal film. The other ends of these two wires were connected to instruments via alligator clips as front contacts. The device had two openings for illumination, and a cell holder was used to position the device so the incident light could hit the surfaces of samples without creating any shadow. Two screws were necessary to hold together the cell device.

2.4.3. The Third-generation MIS Device

The front contact of the second-generation device was replaced with an indium tin oxide (ITO)-coated glass obtained from Delta Technology. To avoid short-circuiting, the ITO-coating was pre-patterned so that the area and the shape of conductive coating match that of the deposited metal on the Si surface. The design for patterning mask was created in ClarisDraw version 1.0.4 and was printed out and photographed onto a Kodak mask plate. At least 30 min prior to the patterning, ITO-coated slides were cleaned in acetone and 18 MΩ·cm H₂O, dried in a stream of N₂(g), and baked in a 100°C oven for 30 min.

This step served to degrease the slide surface and to eliminate moisture, both could affect the adhesion of photoresist.

Shipley 1818 photoresist was spin-coated (~ 30 s) onto the ITO-coated side (cut into $2.5 \text{ mm} \times 2.5 \text{ mm}$ pieces), pre-baked in a 90°C oven for 20 min, and then exposed to UV radiation under the patterning mask for 60 s. After immersing the slides in Shipley CD-30 developer, the UV-exposed part of photoresist was washed off in deionized water. The slides were blow-dried with $\text{N}_2(\text{g})$ and post-baked at 90°C for 15 min. Once the photoresist pattern was baked onto the ITO coating, the uncovered portion was etched away in an aqueous solution of 20% HCl (EM Science) and 5% HNO_3 (EM Science) at 55°C for 5–7 min. The ITO-coated slides were rinsed with $18 \text{ M}\Omega\cdot\text{cm}$ H_2O , and then immersed in a basic solution of 10% Na_2CO_3 to neutralize the acid etch. The slides were again rinsed with $18 \text{ M}\Omega\cdot\text{cm}$ H_2O and dried under $\text{N}_2(\text{g})$. The remaining photoresist was washed off with acetone, followed by another $18 \text{ M}\Omega\cdot\text{cm}$ H_2O rinse and $\text{N}_2(\text{g})$ dried. The ITO pattern could be seen clearly.

The Si samples were cut into $5 \text{ mm} \times 8 \text{ mm}$ pieces and were modified and characterized as described. Immediately following the surface derivatization process, the modified samples were introduced into the evaporator for metal deposition. The Ni (99.994%, Alfa AESAR) was deposited onto the electrodes at a rate of $2\text{--}5 \text{ \AA s}^{-1}$ to a thickness of $\sim 115 \text{ \AA}$ or $\sim 500 \text{ \AA}$ by filament evaporation. The samples used for measurements in the dark only had thicker metal films to prevent short-circuiting. A mask was used to limit the area of deposited Ni to a circular shape with an area of 0.1257 cm^2 , the same size and shape as the patterned ITO front contact. Each cell could hold two samples at the same time (Figure 3.4).

2.4.4. The Fourth-generation MIS Device

The Si samples were modified as described, and $300\text{--}500 \text{ \AA}$ of Ni was deposited on the modified samples by filament evaporation immediately after the derivatization. A

mask was used during the metal deposition to allow a circular shaped metal film of an area of 0.1257 cm^2 . The MIS samples were ohmic contacted on the back surface. As illustrated in Figure 3.5, cell device consisted of a Cu plate that was secured on a plastic base and a thin Rhodium (Rh) wire held steady by an insulated block was used for electrical measurements. The backside of a sample was placed on the Cu plate that served as a back contact with the aid of silver print. The tip of the Rh wire was bent and gently lowered to the front surface of the MIS sample until an electrical contact was made. The Rh wire was very thin and relatively flexible, so that it would not penetrate the metal layer on contact.

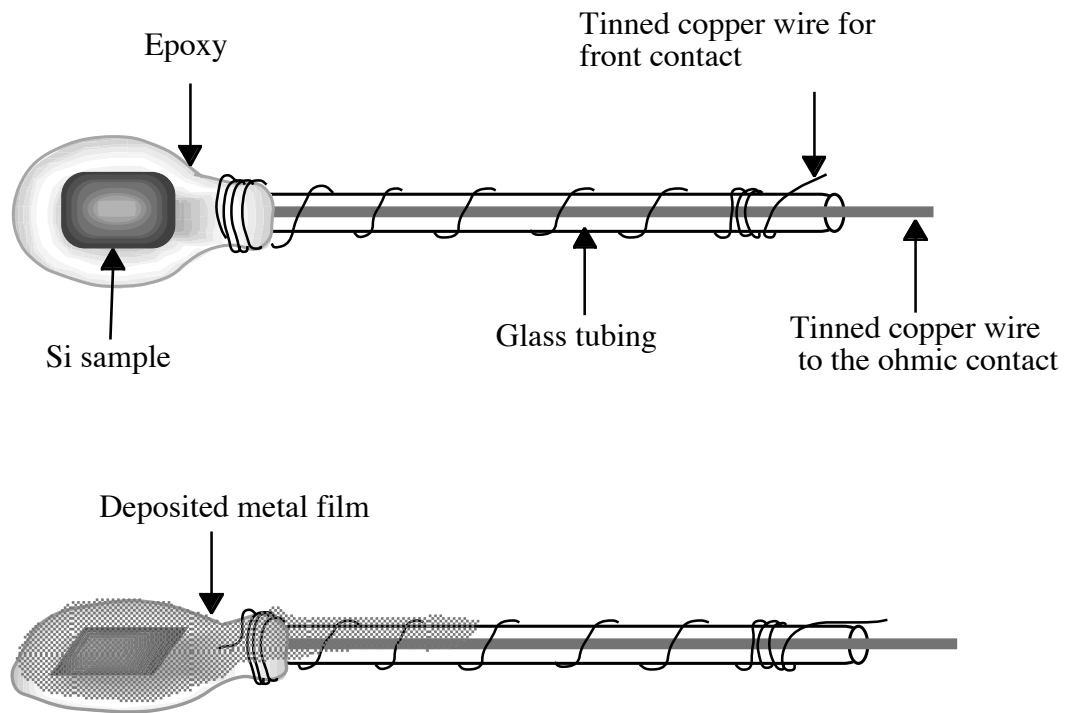


Figure 3.2

An illustration of the first-generation MIS device. The Si sample was first modified with a desired insulating layer, ohmic contacted on the backside, and made into an electrode. A Cu wire bonded to the ohmic contact was used as a back contact, and was covered by insulated epoxy. A thin Cu wire wrapped around the glass tubing was covered with the deposited metal to serve as a front contact. The metal was deposited after the epoxy was allowed to cure for at least 24 hours.

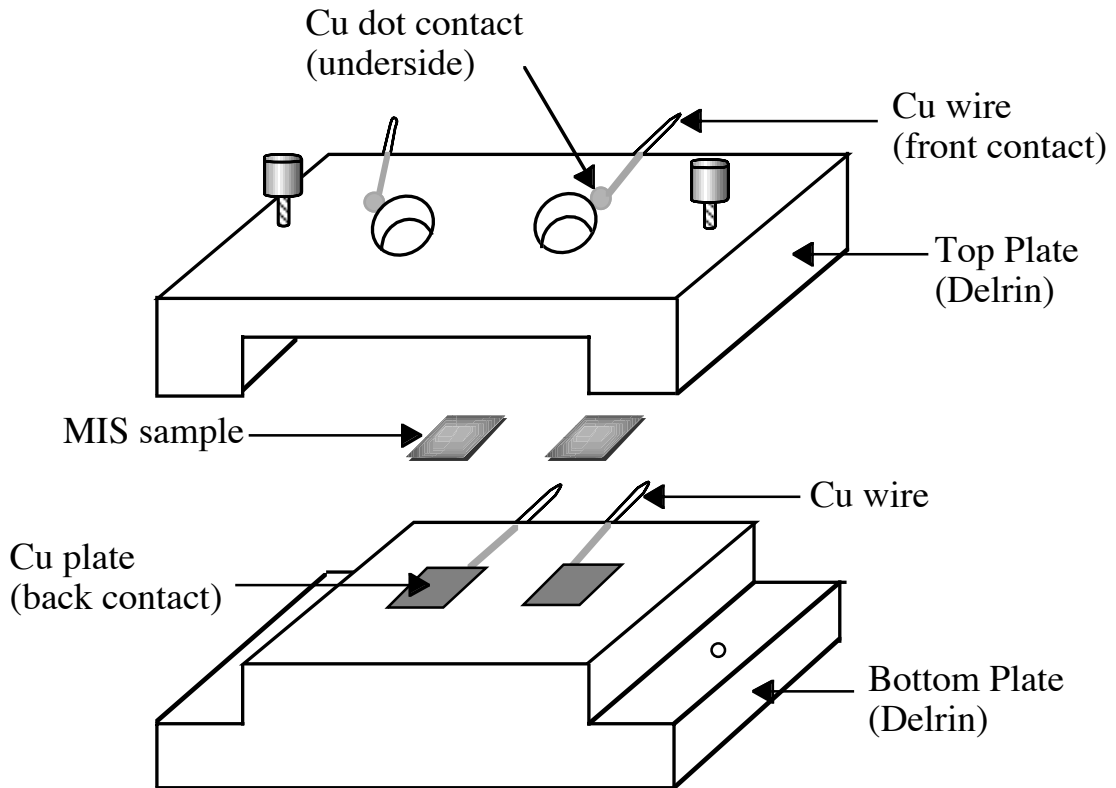


Figure 3.3

An illustration of the second-generation MIS device. The Si surfaces were modified followed by immediate metal deposition to form a MIS sample. The ohmic contacts were made on the backside of samples, silver print was painted on between the ohmic contacts and the Cu plates embedded on the bottom part of the cell. The front contacts were provided by Cu dots embedded in the underside of the cell top plate, which then came in contact with the deposited metal film on these samples. Two samples were sandwiched in a cell held together with two screws.

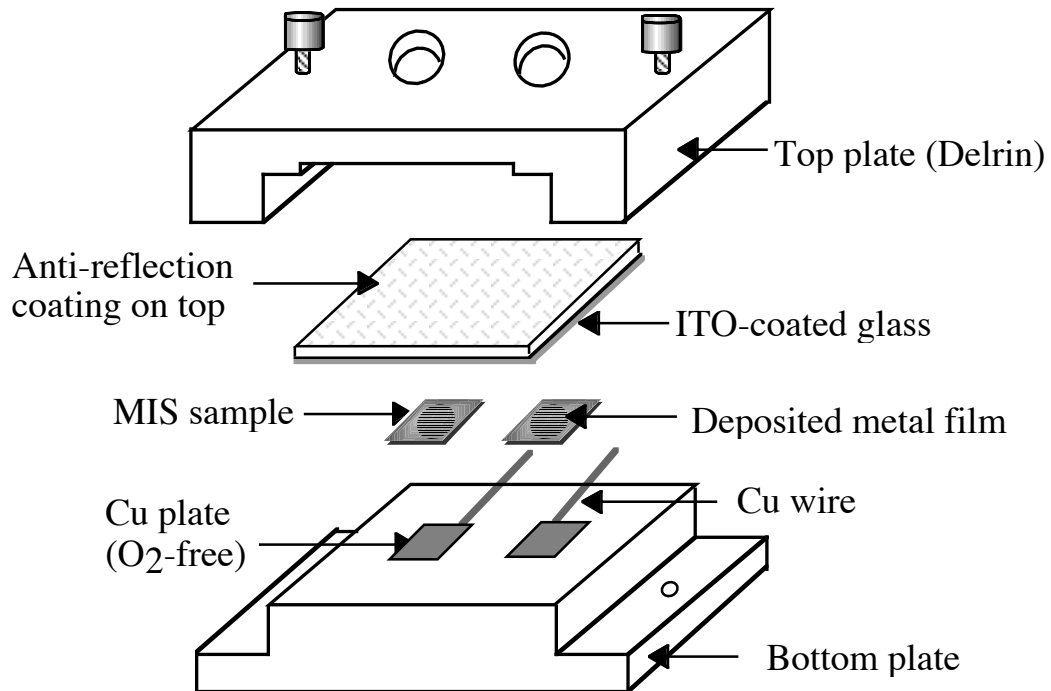


Figure 3.4

An illustration of the third-generation MIS device. The Si surfaces were modified and followed by immediate metal deposition with a mask to define the electrode area. The back contact was made the same way as the second-generation cell. The front contact was made by using pre-patterned ITO-coated glass to make an electrical contact with the deposited metal film. The antireflection coating ensured that the illumination intensity was not greatly affected by the presence of a glass slide. The cell was assembled and held tight with screws, and could hold two MIS samples for electrical measurements.

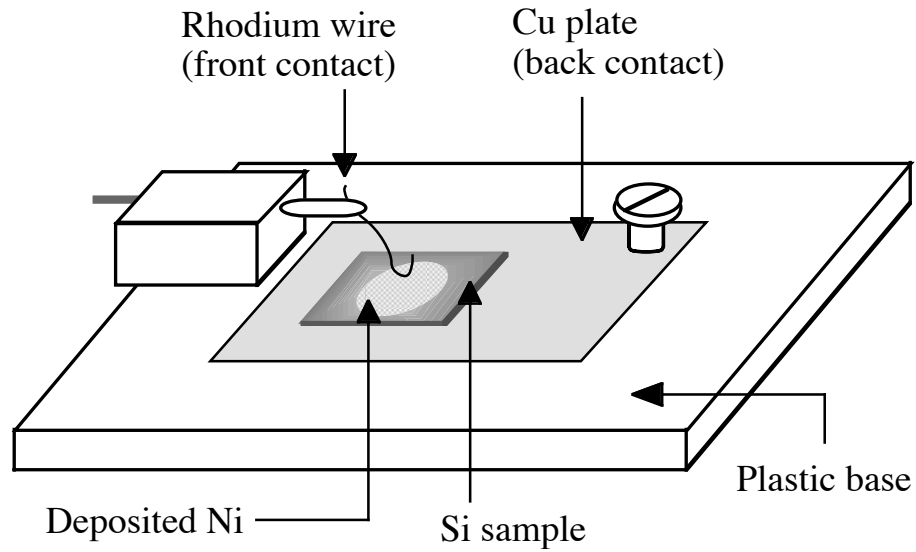


Figure 3.5

An illustration of the fourth-generation MIS device. A large Cu plate secured on a plastic base was used to back contact the MIS sample. A soft flexible Rh wire was gently placed on the deposited metal film for front contact. The ohmic contact of Si was bonded to the Cu plate using silver print. A mask was also used to deposit a metal film of a circular shape with an area of 0.1257 cm^2 .

2.5. Surface Characterization

All surfaces were characterized by x-ray photoelectron spectroscopy (XPS). The experiments were conducted in an M-probe surface spectrometer (VG Instrument) pumped by a CTI Cryogenics-8 cryo pump. Samples could be introduced into the UHV system using either the atmospheric load lock or the glove box load lock. The atmospheric load lock was pumped by a Varian model V80 turbo pump and a Varian model SD-300 mechanical pump, and allowed samples to be introduced into the UHV from air. The glove box load lock was pumped by a Varian model V200 turbo pump and a Varian model SD-300 mechanical pump, and enabled samples to be transferred into the UHV through a gate valve that opened to the N₂(g)-purged glove box. These load locks were brought to the atmospheric pressure by back-filling with N₂(g), and can be pumped down to approximately 10⁻⁷ Torr in about 10 min. Samples were mounted on a stainless steel or aluminum stub with screws.

The XPS chamber was maintained at a base pressure of less than 5 × 10⁻¹⁰ Torr, although the operating pressure was 5 × 10⁻⁹ to 2 × 10⁻⁸ Torr. Monochromatic Al K_α x-rays (hν = 1486.6 eV) incident at 35° from the sample surface were used to excite electrons from the sample, while the emitted electrons were collected by a hemispherical analyzer at a take-off angle of 35° from the plane of the sample surface. Data collection and analysis were done with the M-probe package software version 3.4. Survey scans were collected in the scanned mode with an elliptical spot of dimensions 800 μm × 1200 μm incident on the sample surface. The high-resolution scans were recorded in an unscanned mode with the same spot size. A typical XPS characterization of a surface consisted of one survey scan from 0–700 eV binding energy and a high resolution scan of the Si 2p region (97.57–104.59 eV binding energies).

2.6. Electrical Measurements

Electrical characterization of MIS samples was performed using a two-electrode configuration with the ohmic contact to the back of the Si as the working electrode and the metal contact on the front of the electrode as the counter/reference electrode. The electrodes and cell devices were positioned so that incident light arrived normal to the sample surface.

Current density vs. potential (J - E) measurements were performed using a Solartron Model 1287 potentiostat or an EG&G Princeton Applied Research (PAR) Model 173 potentiostat/galvanostat equipped with an EG&G PAR Model 175 universal programmer. When EG&G PAR Model 173 potentiostat/galvanostat was used, traces were recorded on a Houston Instruments Omnigraphic 2000 chart recorder. All curves were recorded at a scan rate of 100 mV s⁻¹. Light intensities were controlled by the use of a 300 W ENH-type tungsten-halogen bulb in conjunction with neutral density filters (ND-50, Hoya Optics). A 10 cm path-length flowing water column was used to filter out the infrared portion of the lamp output and thereby prevent excess heating of the sample.

The photoresponse experiments involved collecting the photocurrent density (J_{ph}) and the open-circuit voltage (V_{oc}) values at different illumination intensities. Direct measurements of V_{oc} and J_{ph} were taken by reading the appropriate quantities through a Fluke 27 digital multimeter. The reverse saturation current (J_0) and the diode quality factors (γ) of C_nH_{2n+1}-terminated Si ($n = 2-8$) /Ni junctions were obtained.

The current-voltage properties for most semiconductor diodes are found to obey the equation:²³

$$J = J_0 \left[\exp\left(\frac{-qV}{\gamma kT}\right) - 1 \right] \quad (3.2)$$

where $J_0 = A^{**}T^2[\exp(-q\phi_b/kT)]$, q is the charge on an electron, V is the applied potential, γ is the diode quality factor, k is Boltzmann's constant, T is the absolute temperature, and A^{**} is the modified Richardson's constant (for n -Si, $A^{**} \approx 120 \text{ A/cm}^2\cdot\text{K}^2$).²⁴ Dark J - E measurements allow the preparation of a plot of $\ln J$ vs. V , which should give a linear relationship of the form:

$$\ln J \approx \frac{-qV}{\gamma kT} + \ln J_0 \quad (3.3)$$

where J_0 and γ can be extracted from the data. When the diode is under illumination, the current can be described by adding the current from photogenerated carriers to the dark current.^{25,26} Equation 3.11 can be modified to describe the J - E relationship under illumination:

$$J = J_{\text{ph}} - J_0 \left[\exp\left(\frac{-qV}{\gamma kT}\right) - 1 \right] \quad (3.4)$$

At open circuit ($J = 0$), Equation 3.10 is rearranged to yield the following expression:²⁷

$$V_{\text{oc}} \cong \frac{\gamma kT}{q} \ln\left(\frac{J_{\text{ph}}}{J_0}\right) \text{ for } J_{\text{ph}} \gg J_0 \quad (3.5)$$

Following this equation, a photoresponse experiment can also provide an experimental value for both γ and J_0 .

Since most MS diodes are dominated by thermionic emission (i.e., $\gamma = 1$),²⁶ the barrier heights can be calculated from the following:

$$\phi_b = \frac{kT}{q} \ln\left(\frac{A^{**}T^2}{J_0}\right) \quad (3.6)$$

By using metals with different work functions to construct equivalent MS and MIS diodes, a comparison of the two measured barrier heights will allow verification of the effectiveness of the interfacial alkyl layer.

3. Results

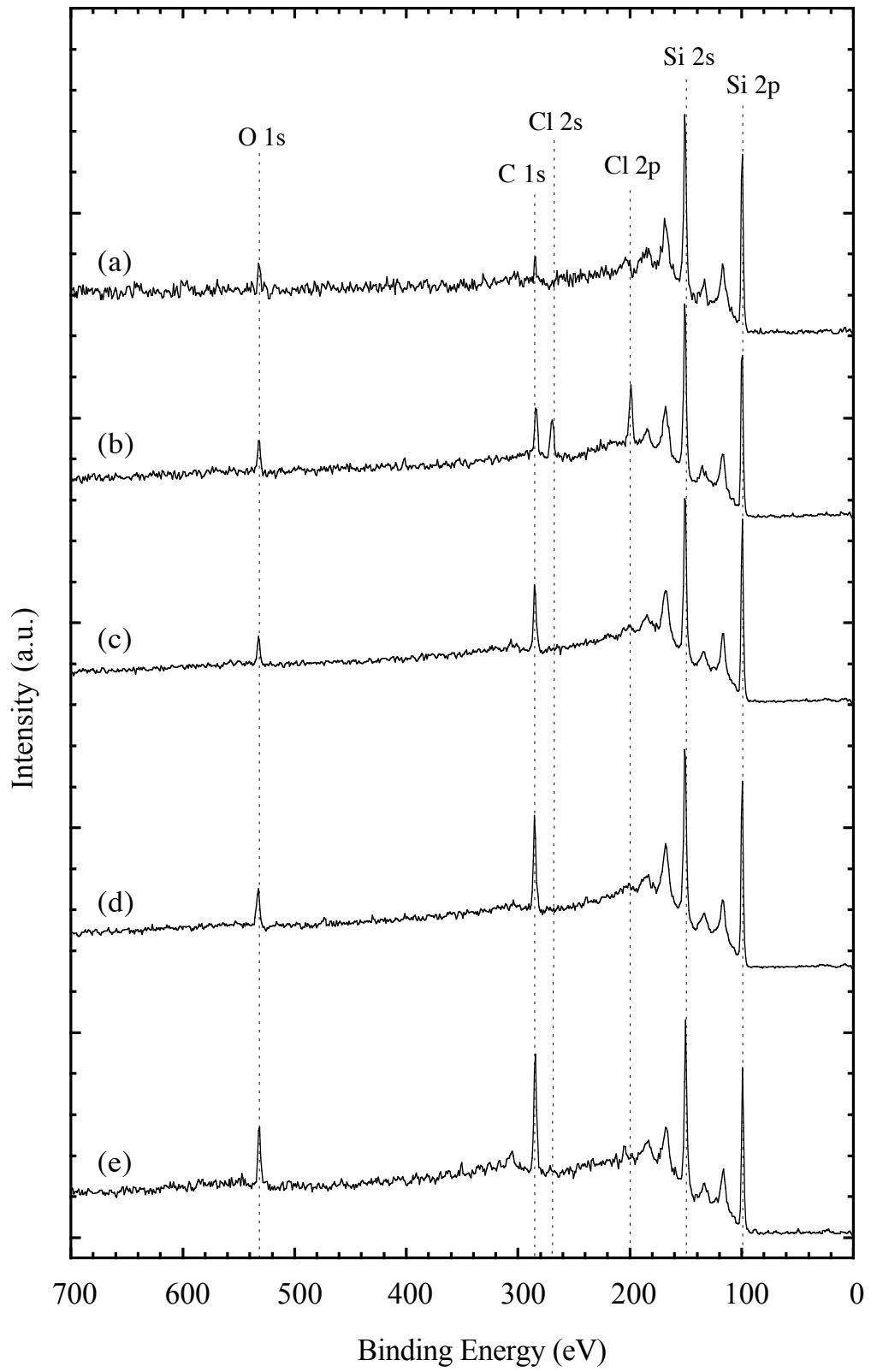
3.1. Surface Modification

The surface modification process was monitored and verified using XPS. Figure 3.6 displays the XP spectra obtained at each step of the surface modification process. A successful etching procedure produced an H-terminated Si surface with a clean spectrum showing large Si 2p and Si 2s peaks at 99 eV and 149 eV binding energies. The smaller peaks present at successive intervals of 17.5 eV binding energy higher than the main Si 2p and 2s peaks were plasmon loss peaks, and were characteristic of Si surfaces.^{28,29} Small signals due to adventitious carbon and oxygen were often observed at 284.6 eV (C 1s) and 532 eV (O 1s). The presence of adventitious carbonaceous material on the silicon surface was a result of wet chemical etching and subsequent brief handling of samples in air.^{30,31} The lack of signal in the 101 to 104 eV region of the Si 2p high-resolution XP spectra collected with each survey scans suggested that the oxygen signal observed in survey spectra was not due to silicon oxide.

Figure 3.6b shows the representative spectrum of a chlorinated Si surface. Additional peaks were observed at 270 eV and 200 eV binding energies, which correspond to Cl 2s and Cl 2p peaks.¹⁶ The subsequent Grignard reaction displaced the surface chlorine atoms, and the alkylated surface was confirmed by the disappearance of the Cl peaks and the concomitant increase in magnitude of the C 1s peak in the XP survey spectrum (Figure 3.6c). For alkyl chain lengths of up to 8 carbons, the modification process was straightforward without complication. However, the attempt to attach decyl groups to the Si surfaces resulted in significant oxide growth during the Grignard reaction.

Figure 3.6

XP survey spectra of (a) H-terminated Si, (b) Cl-terminated Si, (c) C3-terminated Si, (d) C6-terminated Si, and (e) C10-terminated Si. All spectra were normalized relative to the intensity of the Si 2p peak. The small C 1s and O 1s peak in (a) were due to adventitious C and O as a result of wet chemical etching and brief handling in air. Spectra (c)–(e) display the relative intensities of C 1s peak for 3 Si surfaces modified with alkyl chains of different lengths. The C 1s peak intensity generally increases as longer alkyl chains were attached.



3.2. The J - E Behaviors of MIS Diodes

Figure 3.7 display the J - E behaviors of an H-terminated Si/Ni contact and a C_3H_7 -terminated Si/Ni contact, respectively. The measurements were performed using the first-generation device. The introduction of the covalently attached propyl layer showed significant lowering of the J_0 and slight increases in the V_{oc} values at similar J_{ph} . This provided promising result for the concept of making MIS devices using alkyl chains as insulating layers. However, reproducibility in J - E behaviors was not achieved, as J - E curves looked somewhat different from one electrode to another.

The second-generation device did not work very well. The Cu dots did not make good enough electrical contacts with the deposited Ni film. The cell resistance was measured to be as high as 350 Ω . The cell resistance was lowered when silver print was used to aid the front electrical contact, however, due to the small dimension of the Cu dots, the use of silver print was somewhat difficult. In many cases the silver print dripped down the side of the sample and short-circuited the front and the back contact.

The device was modified to incorporate the use of highly conductive ITO-coated slides to make front contacts with MIS samples. This third-generation cell device certainly provided more reliable front contacts. The cell resistance was typically under 60 Ω . Although still suffered from irreproducibility between samples, a set of J - E behavior data was collected using a series of C_nH_{2n+2} -terminated Si ($n = 2, 4, 6, \text{ and } 8$) modified at the same time along with an H-terminated Si. A thin layer of Ni (114 \AA) was deposited on these samples at a rate of $\leq 2.0 \text{ \AA s}^{-1}$. Figure 3.8 displays the J - E properties of these MIS junctions in the dark. The Si-H/Ni junction had a large anodic current at reverse biases indicating a very weak diode behavior due to a large J_0 . With an ethyl layer in between the Si and the Ni, the J - E curve improved significantly, although still exhibited a large reverse saturation current. When the J - E behaviors of C_4H_9 -, C_6H_{13} -, and C_8H_{17} -terminated Si/Ni junctions were plotted together with H- and C_2H_5 -terminated

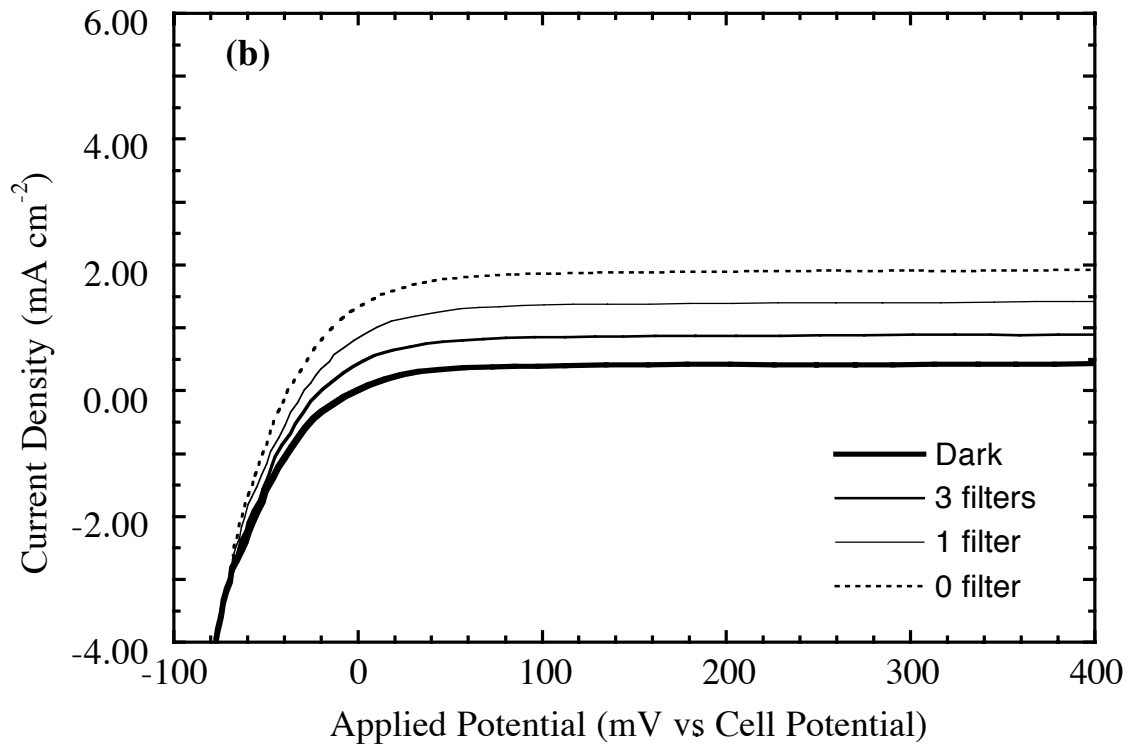
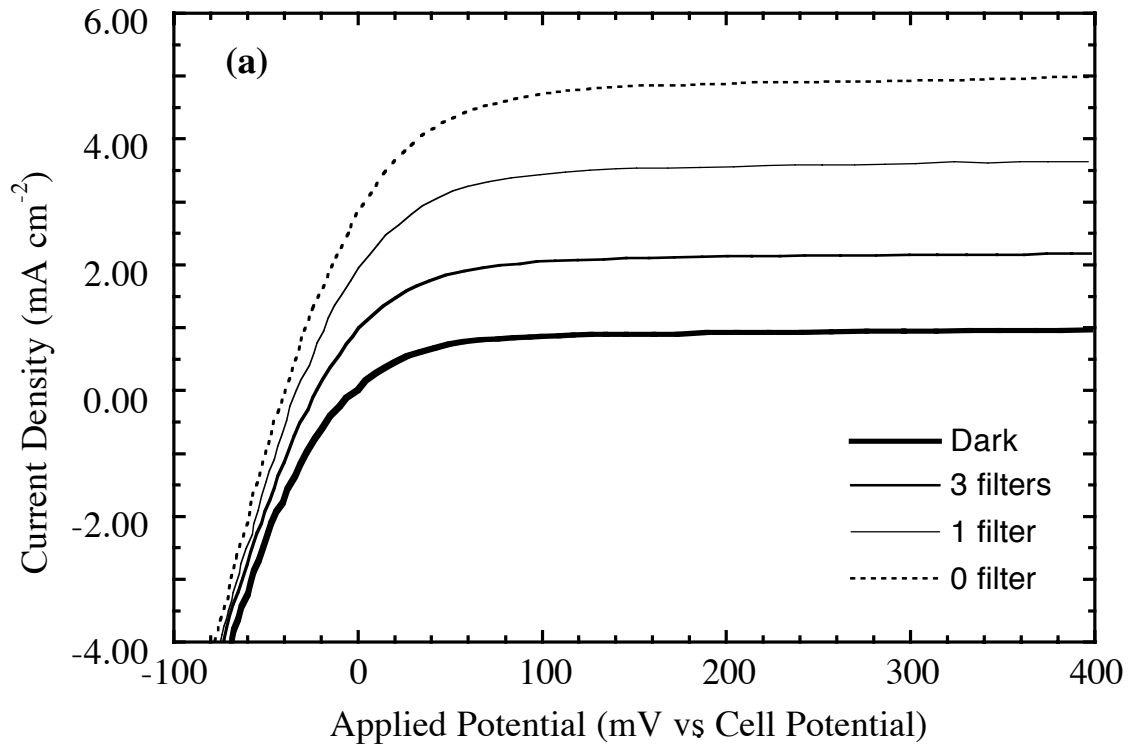
Si/Ni junctions, it was clear that the insulating layers were capable of lowering the J_0 and also resulted in larger V_{oc} values.

The photoresponses of these MIS devices were also measured at several different illumination intensities. The $\ln J_{sc}$ vs. V_{oc} data were plotted in Figure 3.9. Again, the results showed the same effect observed in earlier $J-E$ experiments. The C_8H_{17} -terminated Si/Ni junction was the best choice of all devices tested, with a lower J_0 and higher V_{oc} value compare to the other junctions tested. Because the $J-E$ behaviors of both Si-H and Si- C_2H_5 /Ni junctions did not follow the diode equation, and anodic currents did not level out in the reverse bias region studied, a quantitative calculation was not possible. A time dependence of several C_8H_{17} -terminated Si/Ni junctions $J-E$ behaviors was also performed. The samples were left in the air for 3 days and the $J-E$ curve of each device was collected every 24 hours. As depicted in Figure 3.10, this junction was not air stable and the $J-E$ characteristics deteriorate quickly to show large resistance in the forward bias region.

Since the third-generation device still did not allow reproducible data to be collected, the fourth-generation device that was very similar to the device used for prior MIS study in our laboratory was tested.¹⁵ A larger number of the same surface was made at the same time to insure the same quality control. The attempts to achieve reproducible $J-E$ behaviors for several types of surfaces were unsuccessful.

Figure 3.7

J-E behaviors of (a) H-terminated and (b) C₃H₇-terminated Si in contact with 450 Å of Ni. The plots were collected using the first-generation cell device. The plots were collected at a scan rate of 100 mV s⁻¹. A significant lowering of the anodic currents at reverse biases suggested that the junction recombination current was lowered when an insulating layer was introduced between the Si and the contacting Ni. The illumination intensities were kept the same for both devices.



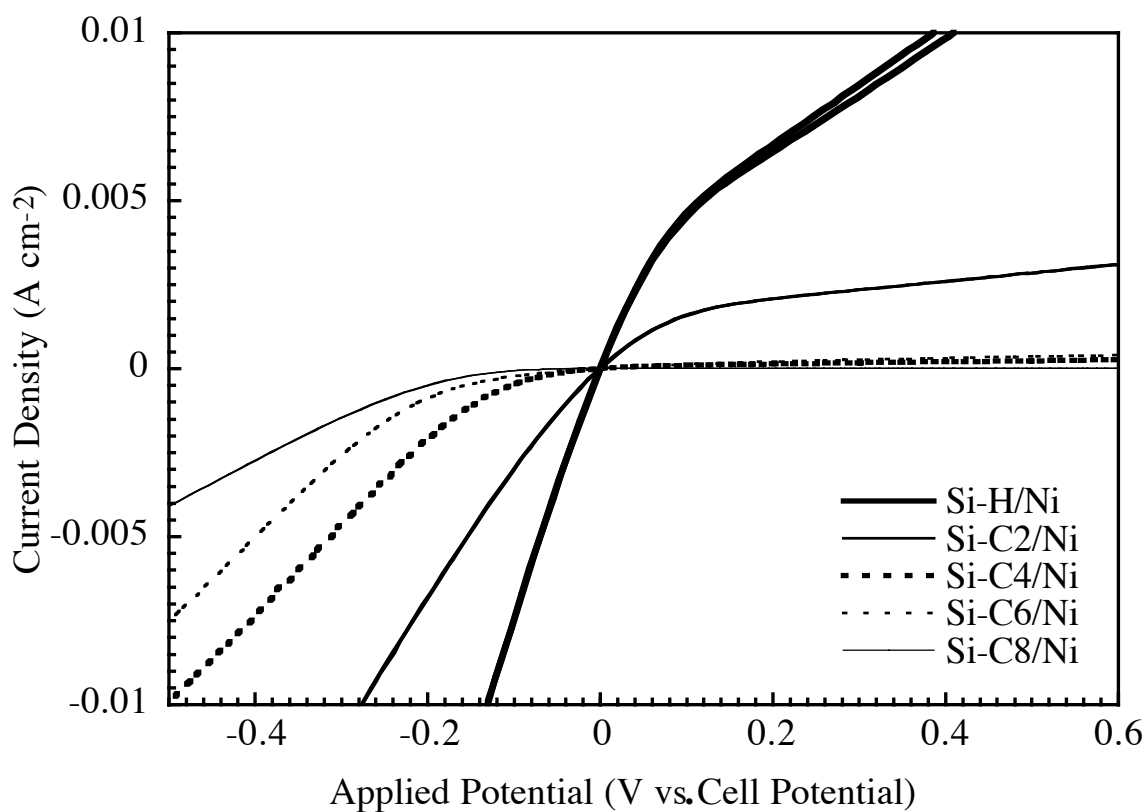


Figure 3.8

J - E behaviors of a series of C_nH_{2n+1} -terminated Si/Ni ($n = 2, 4, 6,$ and 8) and an H-terminated Si/Ni junctions in the dark. The data show the dependence of the MIS junction J - E behavior on the alkyl chain length. The MIS junction with the longest insulator chain length exhibited the lowest anodic current at reverse biases. The MIS diode constructed using a thicker insulator was more resistive at forward bias.

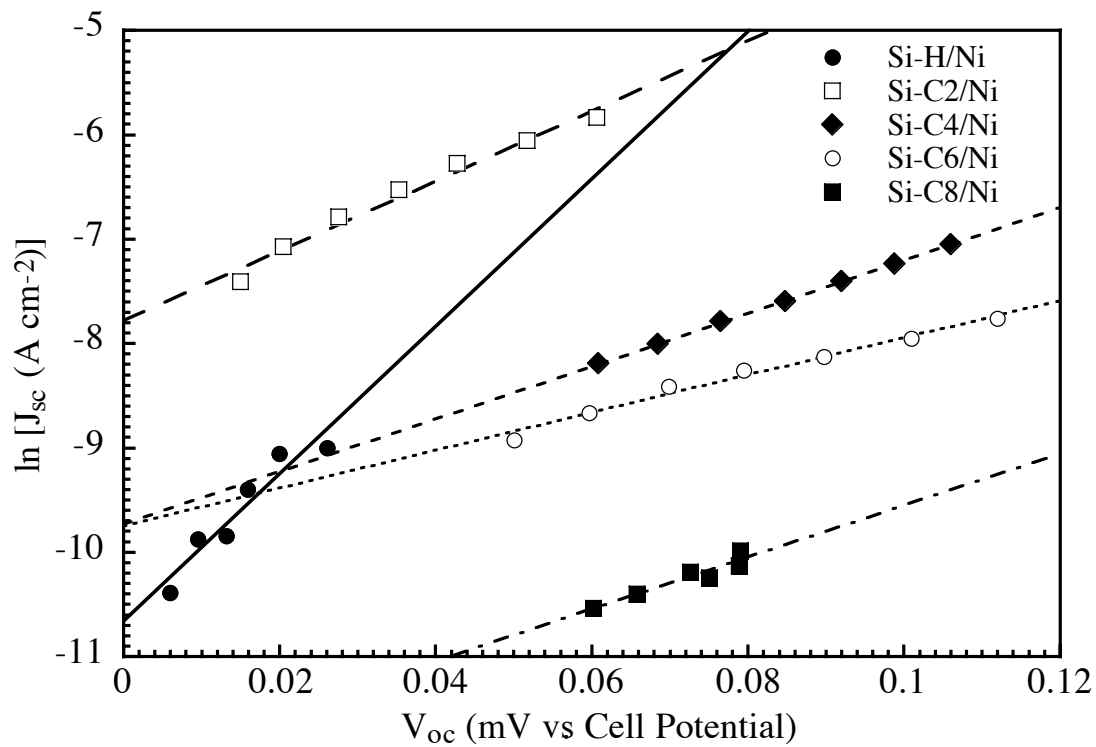


Figure 3.9

Photoresponses of a series of C_nH_{2n+1} -terminated Si/Ni ($n = 2, 4, 6,$ and 8) and an H-terminated Si/Ni junctions. These are plots of the individual photoresponses of the same devices investigated in Figure 3.8.

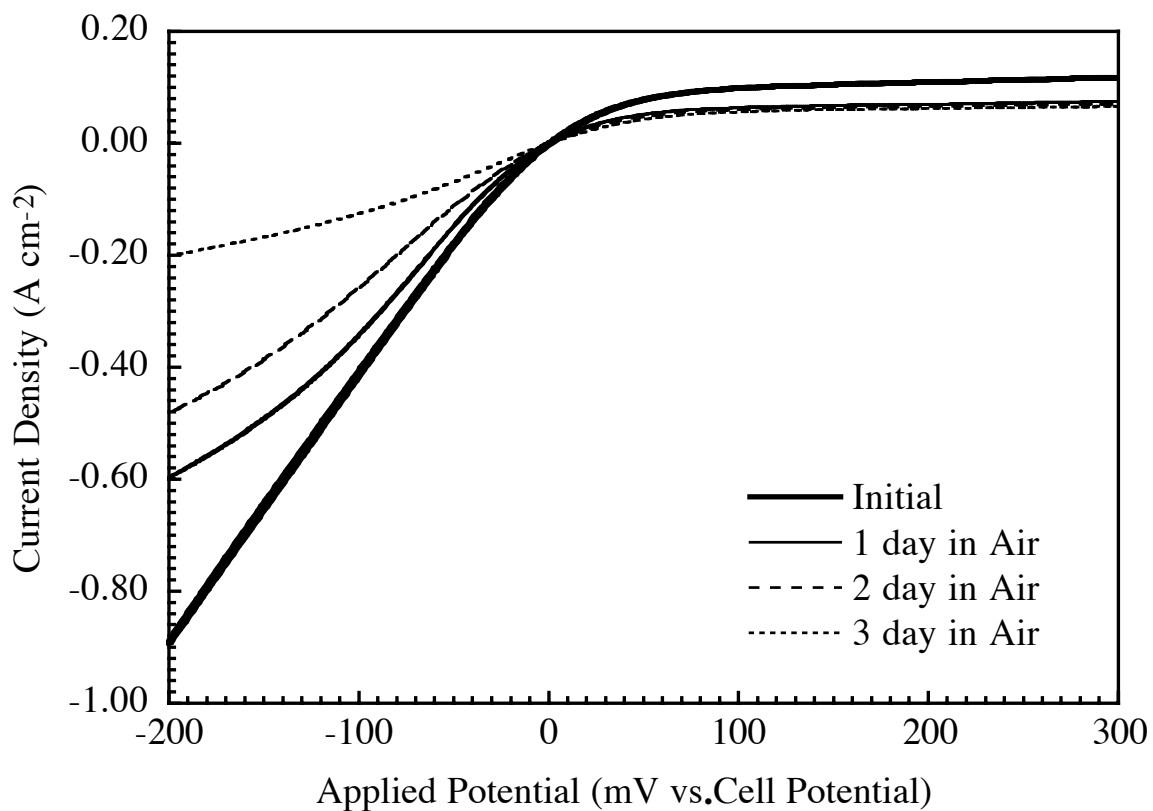


Figure 3.10

Time-dependent $J-E$ behavior of a C_8H_{17} -terminated Si/Ni junction in the dark. The MIS device constructed was not stable in air. The device resistance increased during the course of 3 days, which suggested the possibility of unfavorable interfacial reaction.

4. Discussions

The XPS data confirmed that the two-step chlorination/alkylation method yielded reproducible alkyl overlayer on a Si(111) surfaces. The model suggested that the best possible coverage for an alkylated Si is a half-monolayer coverage (as a 2×1 unit cell), with the exception of methylated surface, which could exhibit one-monolayer coverage. Since the area of the 2×1 unit cell on Si(111) surface is significantly larger than the area required for an alkyl chain in a tightly packed environment, the alkyl overlayer could be quite porous.²² Although the methyl overlayer could provide a better coverage, it was too thin to alter the electrical properties of an H-terminated Si/Ni contact. In fact, the data showed that there was no significant effect when an alkyl chain of shorter than 3 carbons was used as the insulating layer. A longer alkyl chain, on the other hand, could tilt to make the overlayer surface less porous and provide a necessary barrier against silicide formation. However, the possible introduction of an additional series resistance was observed in $J-E$ plots.

The irreproducibility problem could arise from the junction formation process rather than the design of devices for measurements. Thermal evaporation of Ni requires relatively high temperature, and the organic layers on these samples could disintegrate or get damaged under excess heat. The dust could also introduce problems during evaporation and result in inconsistent interfaces. If the metal was deposited in the pin holes or if the hot metal burnt through the organic insulator, the MIS junctions could produce unreliable data, making it difficult to analyze the experimental results quantitatively.

As an alternative to the porosity problem, linear fluorocarbon chains can be used to derivatize the Si surface instead of alkyl chains. The larger head groups of fluorocarbon chains could serve as a blocking layer and might result in a much more

chemically impenetrable coverage, therefore a better barrier against metal penetration in a MIS contact.

Different metal deposition methods can also be investigated. Electroless deposition of gold or nickel onto GaP has been reported to yield almost ideal Schottky diodes.³² Palladium and copper contacts to Si have also been made using an electroless process.^{33,34} Metal-binding agents such as thiols can be incorporated into the monolayer head group, which can in turn bind colloidal Au and Pt.^{35,36} Electrodeposition can also be adapted to plate a metal layer on the alkyl monolayer-Si substrate with a well controlled thickness.^{37,38} There are however other concerns for liquid phase deposition. It is unclear as to how the trapped liquid molecules might affect the electrical properties of the junction. Since the alkyl layer is somewhat porous, the liquid could actually come in contact with Si substrate and either induce oxide growth or allow the metal deposition to occur directly on the Si surface where it's not covered. Electroplating current would prefer to go through the areas with the least resistance, and this could mean that it is easier for metal plating to occur at the sites of pin holes, which again decreases the effectiveness of insulating layer.

Another approach for the fabrication of MIS diodes is mass production of the same junction. By making large batches of junctions for measurements, it would be possible to recognize and discard unreliable data from each set of measurement. This could be achieved by modifying the surfaces of large wafers instead of smaller size samples, followed by depositing metal dots or islands to form a large number of junctions on each modified wafer. Since it is easier to have a smaller area of modified surface to be free of defect than the whole sample surface, those metal dots that were deposited on a region that has no pin hole would be able to provide reliable data for junction characterizations.

Once an effective alkyl monolayer is obtained, different metals should be deposited onto both H-terminated Si and derivatized Si to make equivalent MS and MIS

diodes. In an order of decreasing metal work functions, metals that can be used are Pt, Pd, Au, Rh, Ni, Co, Cu, Cr, Al, and Ag. Pt, Pd, and Au should yield large barrier heights at unpinned metal/*n*-type Si junctions, while Ag, Al, and Cr/*n*-Si interfaces should produce a $V_{oc} \approx 0$ due to theoretically low barrier heights.

5. Summary

Several different chain lengths of alkanes, from methyl to octyl groups, have been successfully attached to the n -Si(111) surface using a two-step chlorination/alkylation method. Contacting Ni layers of thicknesses ranging from 115 Å to 500 Å have been thermally evaporated onto both freshly etched H-terminated and alkyl-terminated Si, and the J - E behaviors of these resulting junctions have been investigated. Introduction of a monolayer with a chain length longer than 4 carbons between the Ni and the Si was shown to consistently lower the value of J_0 while an increase in the values of V_{oc} were observed. A general trend of an increased effectiveness was shown for longer alkyl chains, but the thicker films also introduced larger cell resistances. Although reproducibility of the MIS J - E properties could not be achieved despite the use of several different cell devices, some suggestions were presented for possible future work.

6. Acknowledgments

I thank Reynold Johnson in the Department of Applied Physics for assisting with the photoresist patterning.

7. References

- (1) Braun, F. *Ann. Phys. Chem.* **1874**, 153, 556.
- (2) Sharma, B. L., Ed. *Metal-Semiconductor Schottky Barrier Junctions and Their Applications*; Plenum: New York, 1984.
- (3) Schottky, W.; Stromer, R.; Waibel, F. *Hochfrequenztechnik* **1931**, 37, 162.
- (4) Schottky, W. *Naturwissenschaften* **1938**, 26, 843.
- (5) Mott, N. F. *Proc. Camb. Phil. Soc.* **1938**, 34, 568.
- (6) McGill, T. C. *J. Vac. Sci. Technol.* **1974**, 11, 935.
- (7) Bardeen, J. *Phys. Rev.* **1947**, 71, 717.
- (8) Heine, V. *Phys. Rev. A* **1965**, 138, 1689.
- (9) Schmid, P. E.; Ho, P. S.; Foll, H.; Tan, T. Y. *Phys. Rev. B-Condens Matter* **1983**, 28, 4593.
- (10) Schmid, P. E. *Helv. Phys. Acta* **1985**, 58, 371.
- (11) Rhoderick, E. H.; Williams, R. H. *Metal-Semiconductor Contacts*; 2nd ed.; Oxford University Press: New York, 1988.
- (12) Ottaviani, G.; Tu, K. N.; Mayer, J. W. *Phys. Rev. Lett.* **1980**, 44, 284.
- (13) Freeouf, J. L.; Rubloff, P. S.; Ho, P. S.; Kuan, T. S. *J. Vac. Sci. Technol.* **1980**, 17, 916.
- (14) Andrews, J. M.; Phillips, J. C. *Phys. Rev. Lett.* **1975**, 35, 56.
- (15) Rosenblum, M. D. Ph. D., Stanford University, 1988.
- (16) Bansal, A.; Li, X.; Lauer mann, I.; Lewis, N. S.; Yi, S. I.; Weinberg, W. H. *J. Am. Chem. Soc.* **1996**, 118, 7225.
- (17) Linford, M. R.; Chidsey, C. E. D. *J. Am. Chem. Soc.* **1993**, 115, 12631.
- (18) Linford, M. R.; Fenter, P.; Eisenberger, P. M.; Chidsey, C. E. D. *J. Am. Chem. Soc.* **1995**, 117, 3145.
- (19) Higashi, G. S.; Chabal, Y. J.; Trucks, G. W.; Raghavachari, K. *Appl. Phys. Lett.* **1990**, 56, 656.
- (20) Wyman, D. P.; Wang, J. Y. C.; Freeman, W. R. *J. Org. Chem.* **1963**, 28, 3173.
- (21) Hassler, K.; Koll, W. *J. Organomet. Chem.* **1995**, 487, 223.
- (22) Bansal, A. Ph. D., California Institute of Technology, 1997.
- (23) Sze, S. M. *The Physics of Semiconductor Devices*; 2nd ed.; Wiley: New York, 1981.
- (24) Andrews, J. M.; Lepselter, M. P. *Solid State Elec.* **1970**, 13, 1011.

- (25) Fonash, S. J. *Solar Cell Device Physics*; Academic: New York, 1981.
- (26) Fahrenbruch, A. L.; Bube, R. H. *Fundamentals of Solar Cells: Photovoltaic Solar Energy Conversion*; Academic: New York, 1983.
- (27) Kumar, A.; Wilisch, W. C. A.; Lewis, N. S. *CRC Critical Rev.* **1993**, *18*, 327.
- (28) Stinespring, C. D.; Wormhoudt, J. C. *J. Appl. Phys.* **1989**, *65*, 1733.
- (29) Cheng, K. L. *Japan. J. Appl. Phys.* **1995**, *34*, 5527.
- (30) Tufts, B. J.; Kumar, A.; Bansal, A.; Lewis, N. S. *J. Phys. Chem.* **1992**, *96*, 4581.
- (31) Mende, G.; Finster, J.; Flamm, D.; Schulze, D. *Surf. Sci.* **1983**, *128*, 169.
- (32) Gol'dberg, Y. A.; Posse, E. A.; Tsarenkov, B. V. *Electron. Lett.* **1971**, *7*, 601.
- (33) Datta, A. K.; Ghosh, K.; Mitra, R. N.; Daw, A. N. *Solid-St. Electron.* **1980**, *23*, 99.
- (34) Datta, A. K.; Ghosh, K.; Chowdhury, N. K. D.; Daw, A. N. *Solid-St. Electron.* **1980**, *23*, 905.
- (35) Natan, M. J.; Thackeray, J. W.; Wrighton, M. S. *J. Phys. Chem.* **1986**, *90*, 4089.
- (36) Freeman, R. G.; Grabar, K. C.; Allison, K. J.; Bright, R. M.; Davis, J. A.; Natan, M. J. *Science* **1995**, *267*, 1629.
- (37) Bocking, C.; Christie, I. R. *Inter. Sci. Rev.* **1992**, *17*, 239.
- (38) Searson, P. C. *Solar Energ Mater Solar Cells* **1992**, *27*, 377.